Role of SRP RNA in the GTPase Cycles of Ffh and FtsY[†]

Paul Peluso,[‡] Shu-ou Shan,[‡] Silke Nock,[‡] Daniel Herschlag,[§] and Peter Walter*,[‡]

Howard Hughes Medical Institute and Department of Biochemistry and Biophysics,
University of California at San Francisco, San Francisco, California 94143-0448, and
Department of Biochemistry, B400 Beckman Center, Stanford University,
Stanford, California 94305-5307

Received August 9, 2001; Revised Manuscript Received October 12, 2001

ABSTRACT: The bacterial homologues of the signal recognition particle (SRP) and its receptor, the Ffh•4.5S RNA ribonucleoprotein complex and the FtsY protein, respectively, form a unique complex in which both Ffh and FtsY act as GTPase activating proteins for one another, resulting in the mutual stimulation of GTP hydrolysis by both proteins. Previous work showed that 4.5S RNA enhances the GTPase activity in the presence of both Ffh and FtsY, but it was not clear how this was accomplished. In this work, kinetic and thermodynamic analyses of the GTPase reactions of Ffh and FtsY have provided insights into the role of 4.5S RNA in the GTPase cycles of Ffh and FtsY. We found that 4.5S RNA accelerates the association between Ffh and FtsY 400-fold in their GTP-bound form, analogous to its 200-fold catalytic effect on Ffh•FtsY association previously observed with the GppNHp-bound form [Peluso, P., et al. (2000) *Science 288*, 1640−1643]. Further, Ffh−FtsY association is rate-limiting for the observed GTPase reaction with subsaturating Ffh and FtsY, thereby accounting for the apparent stimulatory effect of 4.5S RNA on the GTPase activity observed previously. An additional step, GTP hydrolysis from the Ffh•FtsY complex, is also moderately facilitated by 4.5S RNA. These results suggest that 4.5S RNA modulates the conformation of the Ffh•FtsY complex and may, in turn, regulate its GTPase activity during the SRP functional cycle.

The signal recognition particle (SRP[1]) is the major cellular machinery that mediates cotranslational targeting of secretory and membrane proteins to the endoplasmic reticulum (ER) membrane in eukaryotic cells or to the plasma membrane in bacteria (*1*). SRP recognizes nascent polypeptide chains that bear N-terminal signal sequences as they emerge from the ribosome (*2*). The complex of ribosome, nascent chain, and SRP is then targeted to the ER or bacterial plasma membrane via interaction of SRP with the SRP receptor (*3*, *4*). Upon this interaction, the ribosome•nascent chain complex is released from SRP and transferred to the translocation machinery, where the protein is either integrated into the membrane or translocated across the membrane to enter, in eukaryotic cells, into the secretory pathway or, in bacteria, into the periplasmic space (*5*).

Targeting by the SRP pathway is evolutionarily conserved (*1* and references therein). Mammalian SRP is a cytosolic ribonucleoprotein complex that consists of six polypeptides and a 7S SRP RNA molecule. The functional core of SRP is the SRP54 protein in complex with the SRP RNA, which recognizes the signal sequence, interacts with the receptor, and binds and hydrolyzes GTP (see below; *6*−*9*). The

bacterial homologues of the SRP54 protein and SRP RNA, Ffh and 4.5S RNA ("R"), comprise a minimal bacterial SRP that can target ribosome•nascent chain complexes to the plasma membrane via interaction with FtsY, the bacterial homologue of the SRP receptor. Thus, the Ffh•R complex and FtsY provide a simplified, biochemically accessible system that allows an in-depth mechanistic investigation of the core features of the targeting process (e.g., *7*, *10*−*13*).

GTP plays a crucial role in the SRP-mediated targeting process (*1*, *14*). Both Ffh and FtsY (and their mammalian homologues) contain GTPase domains that can bind and hydrolyze GTP (*15*−*17*). Although SRP54 lacking its GTPase domain can interact with ribosome•nascent chain complexes, it is unable to target nascent chains to the membrane (*18*). Additional biochemical studies showed that the interaction of Ffh with FtsY requires GTP to be bound to both proteins (*19*, *20*). Upon formation of the Ffh•FtsY complex, both proteins stimulate the GTPase activity of one another (*10*). Finally, hydrolysis of GTP from the Ffh•FtsY

---

* To whom correspondence should be addressed. Phone: 415-476-5017. Fax: 415-476-5233. E-mail: pwalter@biochem.ucsf.edu.

[‡] University of California at San Francisco.

[§] Stanford University.

[1] Abbreviations: SRP, signal recognition particle; Ffh and FtsY, bacterial homologues of the SRP54 protein and the SRP receptor, respectively; R, SRP 4.5S RNA; Ffh•R, complex of Ffh with 4.5S RNA, which comprises a minimal bacterial SRP; Ffh•FtsY, complex between Ffh and FtsY without specifying the nucleotide (GTP, GDP, or GppNHp) bound to the proteins; GTP, guanosine triphosphate; GppNHp, 5′-guanylylimidodiphosphate; GDP, guanosine diphosphate; P_i, inorganic phosphate; XTP, xanthosine triphosphate; HEPES, *N*-[2-hydroxyethyl]piperazine-*N*′-[2-ethanesulfonic acid]; EDTA, ethylenediaminetetraacetic acid; Tris-HCl, tris[hydroxymethyl]aminomethane-hydrochloric acid; PIPES, piperazine-*N*,*N*′-bis[2-ethanesulfonic acid]; IPTG, isopropyl *β*-D-thiogalactopyanoside; PMSF, phenylmethylsulfonyl fluoride; TLC, thin-layer chromatography.

complex is required for dissociation of the complex, allowing the SRP components to be recycled (*21, 22*).

The GTPase domains of Ffh and FtsY define them as members of a unique subfamily of G proteins (*15−17*). Both proteins contain a central GTPase domain that shares homology with other members of the G protein family such as Ras and EF-Tu. An N-terminal helical domain together with this GTPase domain forms a structural and functional unit, called collectively the NG-domain, that is unique for this subfamily of G proteins (*16, 17*). In addition to the NG-domain which is conserved between Ffh and FtsY, each protein possesses a specialized domain that enables it to mediate protein targeting. FtsY has an acidic pre-N-domain, or A-domain, which enables FtsY to interact with the membrane (*23*). Potentially, interaction of this A-domain with phospholipid membranes and possibly with the translocation machinery could modulate the GTPase activity of FtsY (*24, 25*). On the other hand, Ffh possesses a unique C-terminal methionine-rich domain, or M-domain, which contains the binding pocket for signal sequences (*6, 9, 26, 27*). A positively charged helix-turn-helix motif in the M-domain also provides the binding site for the SRP RNA (*8, 9, 27, 28*). Communications between the M- and NG-domain presumably occur during the targeting pathway to allow the cycle of signal sequence binding/release and the cycle of GTP binding/hydrolysis to be coupled to one another.

While early biochemical studies identified specific functional roles for the different protein subunits (*1* and references therein), the SRP RNA appeared to be nothing more than a scaffold that holds these proteins together in a complex (*29*). The identification of 4.5S RNA, a smaller SRP RNA in *Escherichia coli* that binds only a single protein, was therefore intriguing. This smaller RNA contains the most phyllogenetically conserved region of the SRP RNA, domain IV, which is likely to have been maintained for functional purposes (*30, 31*). Moreover, chemical probing studies showed that many of the bases in domain IV are highly solvent accessible even in the presence of Ffh, suggesting that this domain might be used to interact with another component of the targeting pathway (*32*).

The role for 4.5S RNA has since been the subject of much investigation and discussion. Initially, 4.5S RNA was thought to be required for the formation of the Ffh•FtsY complex (e.g., *20, 33*). However, studies of the *Mycoplasma mycoides* SRP components suggested that the SRP RNA was not essential for the formation of the Ffh•FtsY complex and subsequent stimulated GTP hydrolysis, although the GTPase activity of the Ffh•FtsY complex was suboptimal in the absence of the RNA (*34*). Recently, kinetic studies of the Ffh•FtsY interaction using the GTP analogue, GppNHp, have demonstrated a novel catalytic role for the 4.5S RNA in the formation of the Ffh•FtsY complex. These experiments showed that 4.5S RNA accelerates both the association and dissociation rate constants of Ffh and FtsY by 200-fold, without affecting their equilibrium affinity (*35*). These observations suggest that Ffh and/or FtsY undergo intricate conformational rearrangements during complex formation and that 4.5S RNA may facilitate these changes.

These previous findings indicate that 4.5S RNA plays a crucial role in the SRP-mediated targeting process and raises additional questions. How does the ability of 4.5S RNA to facilitate complex formation relate to its stimulatory effect on the GTPase activity in the presence of Ffh and FtsY? Are there additional steps in the reaction pathway that are affected by 4.5S RNA? More fundamentally, interpretation of an observed effect of 4.5S RNA relies on knowledge of the process that is followed under the particular experimental condition and the rate-limiting step for that process. For instance, with subsaturating proteins the reaction ^{GTP}•Ffh + FtsY•^{GTP} → products is monitored; under these conditions, formation of the protein complex, a conformational change within the complex, or the chemical step of GTP hydrolysis could be rate-limiting. In contrast, the use of saturating protein concentrations allows the reaction ^{GTP}•Ffh•FtsY•^{GTP} → products to be followed, so that complex formation is no longer rate-limiting. Finally, the observed GTPase rate could also be limited by product dissociation in multiple turnover reactions.

To address these issues, we have measured the microscopic rate and equilibrium constants for the GTPase cycles of Ffh and FtsY and determined the effect of 4.5S RNA on individual reaction steps. We show herein that 4.5S RNA enhances the rate of Ffh•FtsY complex formation with GTP bound to both proteins. Further, kinetic analyses of the GTPase cycles indicate that formation of the Ffh•FtsY complex is the rate-limiting step for the observed GTPase reaction with subsaturating protein, thus accounting for the apparent effect of 4.5S RNA in stimulating the GTPase reaction observed previously. 4.5S RNA also has a modest effect on an additional step, the rate of GTP hydrolysis once the complex is formed, suggesting that the RNA favors a conformation of the Ffh•FtsY complex that is more conducive to GTP hydrolysis.

MATERIALS AND METHODS

Buffers. The following buffers are used in the experiments described herein: buffer A (20 mM potassium HEPES, pH 8.0, 2 mM sodium EDTA, 2 mM dithiothreitol), buffer B (50 mM Tris-HCl, pH 7.5, 1 mM disodium EDTA, 2 mM dithiothreitol), buffer C (20 mM potassium acetate, pH 4.7), buffer D (20 mM potassium PIPES, 500 mM potassium acetate, 1 mM magnesium acetate, pH 6.8), and buffer E (50 mM potassium HEPES, 150 mM potassium acetate, 1.5 mM magnesium acetate, 0.01% Nikkol, 2 mM dithiothreitol, pH 7.5).

Ffh Expression and Purification. Ffh was overexpressed from the pDMF6 plasmid in BL21(DE3)-pLysE cells (Stratagene). Cells were grown to a density of $A_{600} = 0.5−0.7$, at which point IPTG was added to a final concentration of 1 mM. About 3−5 h after induction, cells expressing Ffh were harvested, resuspended in buffer A containing 250 mM NaCl and 200 μM PMSF, and lysed by sonication. Supernatant from the cell lysate was loaded onto an SP-Sepharose fast-flow column, washed with 10 column volumes of buffer A containing 250 mM NaCl, and eluted in buffer A with a 250−750 mM NaCl gradient. The Ffh-containing fractions were pooled and precipitated with 80% ammonium sulfate and dialyzed against buffer A containing 250 mM NaCl. Following a high-speed centrifugation to remove insoluble matter, Ffh was further purified over a Superose-12 column in buffer A containing 250 mM NaCl. The Ffh-containing fractions were pooled and concentrated using Centriprep YM-30 (Amicon) following the manufacturer's instructions.

Purified Ffh was stored at −20 °C in buffer A containing 250 mM NaCl and 50% glycerol. The concentration of Ffh was determined by Bradford assays using an extinction coefficient of $1.0A_{595} = 4.8 \mu M$ Ffh, derived from quantitative amino acid analysis.

FtsY Expression and Purification. A truncation mutant of FtsY, FtsY(47-497), was used in this study. The cloning, expression, and purification of this protein have previously been described (24). One additional purification step was added in the present study. As a final step in the purification, FtsY was loaded onto a MonoQ column (Pharmacia), washed with buffer B containing 150 mM NaCl, and eluted with buffer B over a gradient of 150−450 mM NaCl. Purified FtsY was stored at −80 °C in buffer B containing 250 mM NaCl and 20% glycerol. The concentration of FtsY was determined from Bradford assays using an extinction coefficient of $0.063A_{595} = 1 \mu g/mL$ FtsY, derived from quantitative amino acid analysis.

4.5S RNA Expression and Purification. DH5α cells containing the pSN1 plasmid (36) were grown to saturation in LB containing ampicillin (100 μg/mL) and IPTG (1 mM). Cells were harvested, resuspended in buffer C, and extracted three times with an equal volume of acid phenol:chloroform (Ambion). The RNA was then precipitated by addition of 0.1 vol 3 M sodium acetate (pH 5.0) and 0.6−1.0 vol 2-propanol at −20 °C overnight. The precipitated RNA was harvested by centrifugation at 10 000g, and the pellet was resuspended in water. At this stage, the only major contaminant was tRNA present in similar amounts relative to 4.5S RNA; this contaminant was removed by gel filtration with a TSK3000SW column in buffer D. The 4.5S RNA fractions were pooled and extracted twice with phenol/chloroform, precipitated in ethanol, and stored as ethanol precipitates at −20 °C. The concentration of 4.5S RNA was determined from the absorbance at 260 nm, using an extinction coefficient of $1.0A_{260} = 40 \mu g/mL$ (37).

Buffer Exchange of Ffh and FtsY. All the functional assays described herein were carried out in buffer E unless otherwise specified. Ffh and FtsY were exchanged into buffer E using Bio-Gel P-6 DG spin columns (BioRad) following the manufacturer's instructions. Prior to functional assays, buffer-exchanged protein samples were centrifuged at 300 000g in a TLA100 rotor for 1 h to remove potential aggregates, and the concentrations of the resulting protein solutions were determined using the Bradford assay as described above.

General Kinetic Analysis for the GTPase Reaction. GTPase reactions were performed at 25 °C using α-^{32}P-GTP or γ-^{32}P-GTP (GTP*) in buffer E. Reactions were initiated by addition of GTP. At specified times, an aliquot was removed from the reaction mixture and quenched in 0.75 M potassium phosphate, pH 3.3. Reaction substrates and products were separated by thin-layer chromatography (TLC; PEI Cellulose F). For α-^{32}P-GTP, 0.75 M potassium phosphate (pH 3.3) was used; for γ-^{32}P-GTP, 1 M lithium chloride/0.3 M sodium phosphate (pH 3.8) was used. The developed TLC plates were quantified using a Molecular Imager System GS-363 (BioRad) or a Molecular Dynamics Storm 840.

The basal GTPase activities of Ffh and FtsY were measured in single turnover reactions, with trace amounts of GTP* (<0.1 nM) and excess protein (≥10 nM). These reactions can typically be followed to ≥90% completion,

and the reaction time courses fit well to eq 1, in which Frac-(S) is the fraction of GTP* at each time point, a is the fraction

$$\text{Frac}(S) = (a - b) \exp(-k_{\text{obsd}}t) + b \qquad (1)$$

of GTP* at the beginning of the reaction, b is the fraction of GTP* at the reaction plateau ($t \rightarrow \infty$), and k_{obsd} is the observed rate constant of the reaction. The slow reactions were typically linear for up to 24 h, and the reaction time courses were fit to eq 1 assuming an endpoint of $b = 0.1$, the endpoint usually observed in reactions that can be followed to completion.

The GTPase rate in the presence of both Ffh and FtsY needed to be measured by multiple turnover reactions, as described in the text. For these reactions, an excess of GTP doped with trace amounts of GTP* was used. The initial linear portion of the time course, in which ≤15% of GTP has reacted, was fit to eq 1 assuming an endpoint of $b = 0.1$.

To know what situations could give rise to a burst phase in the multiple turnover reaction shown in Figure 8, the time course of this reaction was also fit to eq 2, in which a is the amount of GTP hydrolyzed during each turnover, k_1 is the

$$[\text{GTP}] \text{ hydrolyzed} = a[(1 - e^{-k_1 t}) + k_2 t] \qquad (2)$$

reaction rate during the first turnover, and k_2 is the steady-state reaction rate during subsequent turnovers. The value of a was fixed at 40 μM, twice the concentration of the Ffh•FtsY complex available during this experiment, because two GTPs are hydrolyzed from the Ffh•FtsY complex during each turnover. The values of k_1 were fixed at 5-, 10-, and 20-fold relative to that of k_2 in the fits shown in Figure 8. Similar results were obtained from the simulation of the time course of this reaction, in which we varied the relative values of k_1 and k_2 but fixed all of the other rate and equilibrium constants for GTP binding to Ffh and FtsY and for Ffh−FtsY association that have been determined independently (not shown; Berkeley Madonna v8.0)

Determination of GTP and GDP Affinities. The affinity of Ffh and FtsY for GTP can be determined from the dependence of the observed reaction rate on protein concentration according to eq 3. In this equation, k_{obsd} is the observed rate constant at a particular protein concentration,

$$k_{\text{obsd}} = k_{\text{max}} \times \frac{[\text{Ffh}]}{K_{1/2} + [\text{Ffh}]}$$

$$\text{or } k_{\text{obsd}} = k_{\text{max}} \times \frac{[\text{FtsY}]}{K_{1/2} + [\text{FtsY}]} \qquad (3)$$

k_{max} is the maximal rate constant with saturating protein, and $K_{1/2}$ is the protein concentration that provides half the maximal rate. Because the chemical step is rate-limiting for the basal GTPase reactions (see Results), k_{max} is equal to the rate constant for the reaction of the $^{\text{GTP}}$•Ffh or FtsY•$^{\text{GTP}}$ complex, and $K_{1/2}$ is equal to the dissociation constant of GTP for Ffh or FtsY.

The affinity of GDP for Ffh was determined by inhibition methods (eq 4). The observed rate constant of the reaction Ffh + GTP* → products (k_{obsd}) was determined at varying GDP concentrations, and the [GDP]-dependence was fit to

eq 4b, derived from the model of eq 4a. In eq 4b, k_0 is the rate of the reaction in the absence of GDP, and K_i is the inhibition constant of GDP. With subsaturating Ffh, K_i is equal to the equilibrium dissociation constant of GDP.

$$\text{Ffh} + \text{GTP*} \xrightarrow{k_0} \text{products}$$
$$K_i \updownarrow \pm \text{GDP}$$
$$^{\text{GDP}}\text{Ffh}$$
(4a)

$$k_{\text{obsd}} = k_0 \times \frac{K_i}{[\text{GDP}] + K_i}$$
(4b)

Determination of the Rate Constant for Ffh−FtsY Association. Ffh−FtsY association was monitored using a fluorescence assay described previously (*12, 35*). All experiments were performed in a Kintec stopped-flow apparatus at 25 °C in buffer E. Reactions were initiated by rapidly mixing the proteins with 1 mM GTP•Mg^{2+}, and the time course for the change in tryptophan fluorescence of FtsY was monitored to obtain the observed rate constants at varying Ffh concentrations (k_{obsd}). The [Ffh]-dependence of k_{obsd} values was fit to eq 5, in which k_4 is the rate constant for association of $^{\text{GTP}}$•Ffh with FtsY$^{\bullet\text{GTP}}$, k_{-4} is the rate constant for dissociation of the $^{\text{GTP}}$•Ffh•FtsY$^{\bullet\text{GTP}}$ complex, and k_5 is the rate constant for hydrolysis of GTP from the complex, as formation of the $^{\text{GDP}}$•Ffh•FtsY$^{\bullet\text{GDP}}$ leads to the loss of fluorescence (see Figure 1 below).

$$k_{\text{obsd}} = k_4[\text{Ffh}] + k_{-4} + k_5$$
(5)

Determination of the Rate Constant for Disassembly of the $^{\text{GTP}}$•Ffh•FtsY$^{\bullet\text{GTP}}$ Complex. The apparent disassembly of the $^{\text{GTP}}$•Ffh•FtsY$^{\bullet\text{GTP}}$ complex was monitored from the disappearance of the fluorescence signal from this complex and was carried out in a Kintec stopped-flow apparatus at 25 °C. The rate constant of this process was determined by a pulse-chase experiment depicted in eq 6a (*38*). The complex between Ffh and FtsY is first formed in the presence of GTP during t_1. At varying times, t_2, a 50-fold excess of GDP•Mg^{2+} is then added to trap any protein that has dissociated. The time course of the reaction during t_2 was fit to eq 6b, in which F_{obsd} is the observed fluorescence at a given time during t_2, F_0 is the fluorescence before the addition of chase, $F_{t\to\infty}$ is the fluorescence level at the plateau, and k_{obsd} is the observed rate constant for disassembly of the complex.

$$^{\text{GTP}}\text{Ffh} \qquad \text{FtsY}^{\bullet\text{GTP}}$$
(6a)
$$t_1 \qquad \text{GDP•Mg}^{2+} \text{ (chase)}$$
$$t_2$$

$$F_{\text{obsd}} = (F_0 - F_{t\to\infty}) \exp(-k_{\text{obsd}}t) + F_{t\to\infty}$$
(6b)

Determination of the Rate Constant for GTP Hydrolysis from the Complex. The rate constant for GTP hydrolysis was determined in multiple turnover reactions in the presence of a small fixed amount of Ffh and varying concentrations of FtsY, as described in the Results. The [FtsY]-dependence

FIGURE 1: Reaction scheme for the GTPase cycles of Ffh and FtsY. Each enzymatic species (Ffh, FtsY, or the Ffh•FtsY complex) is highlighted by the circles, with superscripts depicting the nucleotide cofactor bound to the protein and ±R denoting the presence or absence of 4.5S RNA. The triangular cycles on the top left and right depict the basal GTPase cycles of Ffh and FtsY, respectively, with K_1 and K_1' denoting the GTP dissociation constants, k_2 and k_2' denoting the rate of GTP hydrolysis, and K_3 and K_3' denoting the GDP dissociation constants for Ffh and FtsY, respectively. Formation of the complex between $^{\text{GTP}}$•Ffh and FtsY$^{\bullet\text{GTP}}$ is characterized by the association rate constant k_4 and the dissociation rate constant k_{-4}. The two bound GTPs are hydrolyzed from the $^{\text{GTP}}$•Ffh•FtsY$^{\bullet\text{GTP}}$ complex, which is represented collectively by a rate constant k_5.[2] The $^{\text{Pi•GDP}}$•Ffh•FtsY$^{\bullet\text{GDP•Pi}}$ complex then dissociates with a rate constant k_6.

of the observed rate constant was fit to eq 2 described above. Unlike the situation in the basal GTPase reactions, dissociation of the $^{\text{GTP}}$•Ffh•FtsY$^{\bullet\text{GTP}}$ complex is slower than hydrolysis of GTP from this complex, as described in the Results. Therefore, the $K_{1/2}$ value obtained is most likely larger than the equilibrium dissociation constant of the complex. On the other hand, the maximal rate constant, k_{max}, is equal to the rate constant for GTP hydrolysis from the complex because product release is most likely not rate-limiting (see Results). This rate constant could still be limited by a conformational change prior to GTP hydrolysis or by the actual chemical step.

RESULTS

Figure 1 depicts the individual microscopic steps in the GTPase reaction cycle of Ffh and FtsY that could potentially be affected by 4.5S RNA. Each of these proteins can bind and hydrolyze GTP without forming a higher-order complex (steps 1−3 for Ffh and 1′−3′ for FtsY). Ffh and FtsY, in their GTP-bound forms ($^{\text{GTP}}$•Ffh and FtsY$^{\bullet\text{GTP}}$, respectively), associate with one another to form the $^{\text{GTP}}$•Ffh•FtsY$^{\bullet\text{GTP}}$ complex (step 4). GTP is then hydrolyzed by both proteins to yield the $^{\text{GDP•Pi}}$•Ffh•FtsY$^{\bullet\text{GDP•Pi}}$ complex (step 5),[2] which then dissociates into the individual protein components (step 6). For simplicity, an alternative pathway for product dissociation, in which GDP and/or P_i first dissociates from

the individual proteins followed by dissociation of the Ffh•FtsY complex, is not depicted. This simplification does not affect the conclusions from this study, because product dissociation is most likely not rate-limiting (see below).

We have determined the rate and equilibrium constants for these individual steps in the presence and absence of 4.5S RNA (depicted by the symbol ±R). An NH$_2$-terminally truncated version of FtsY (residues 47-497) was used in this study. This truncated protein can interact with Ffh and bind and hydrolyze GTP in manners analogous to those of the full-length FtsY (*24*; see results below and Shan, S., unpublished results). However, the higher solubility of this truncated protein allowed us to vary the FtsY concentration over a wider range than is possible with full-length FtsY.

We first show that the RNA has no effect on the basal GTPase cycles of Ffh and FtsY. An effect of 4.5S RNA on formation of the ^{GTP}•Ffh•FtsY$^{•GTP}$ complex is then described. The next section presents results that strongly suggest that GTP hydrolysis from the ^{GTP}•Ffh•FtsY$^{•GTP}$ complex is faster than dissociation of this complex; these experiments also show that the 4.5S RNA has an additional effect on the rate of GTP hydrolysis once the complex is formed. Finally, we describe experiments that strongly suggest that product dissociation is not rate-limiting for the GTPase reaction of the ^{GTP}•Ffh•FtsY$^{•GTP}$ complex, so that the observed effects of 4.5S RNA are unlikely to be exerted on these steps.

4.5S RNA Does Not Affect the Basal GTPase Activity of Ffh. We first asked whether 4.5S RNA affects the GTP affinity and/or hydrolysis rate of Ffh (Figure 1, steps 1−3). To determine more accurately the low basal GTPase activity and to avoid complications from rate-limiting product dissociation, single turnover experiments were performed in which the reaction can be followed to completion (Figure 2). The observed rate constants were plotted as a function of the concentration of Ffh or Ffh•R[3] (Figure 3A). The concentration dependences are the same, within error, in the presence and absence of the 4.5S RNA (open vs closed symbols), indicating that the RNA has no effect on the basal GTPase activity of Ffh.

Analysis of these concentration dependences gave maximal rate constants (k_{max}) of 0.093 and 0.092 min^{-1} and $K_{1/2}$ values (the concentration of Ffh or Ffh•R that provides the half-maximal rate) of 0.31 and 0.30 μM in the presence and absence of 4.5S RNA, respectively. The following strongly suggest that the chemical step, rather than GTP binding, is rate-limiting for the basal GTPase reactions of Ffh: (i) the second-order rate contant for the reaction GTP* + Ffh (or Ffh•R) → products is 10^2-fold slower than the rate of GTP

---

[2] Step 5 represents the hydrolysis of two GTP molecules from the ^{GTP}•Ffh•FtsY$^{•GTP}$ complex, and this step is denoted collectively with a rate constant k_5. Studies using an XTP-specific mutant of FtsY, FtsYD449N, have shown that the maximal rate of GTP and XTP hydrolysis is similar with the Ffh/FtsYD449N combination (*10*). This suggests that the two GTPs are hydrolyzed with the same apparent rates, one from each protein within the complex. It is possible that each protein hydrolyzes a GTP with the rate constant $k_5/2$ within the complex; alternatively, k_5 may represent a rate-limiting conformational change of the complex prior to fast hydrolysis of both GTPs.

[3] 4.5S RNA binds to Ffh with a dissociation constant of 5 nM (*1*). To ensure that all of the Ffh molecules are in the RNA-bound form in experiments that measure the rates or equilibrium for reactions of Ffh•R, at least 100 nM 4.5S RNA was used for Ffh concentrations below 100 nM, and a 2-fold excess of 4.5S RNA was used for Ffh concentrations above 100 nM.
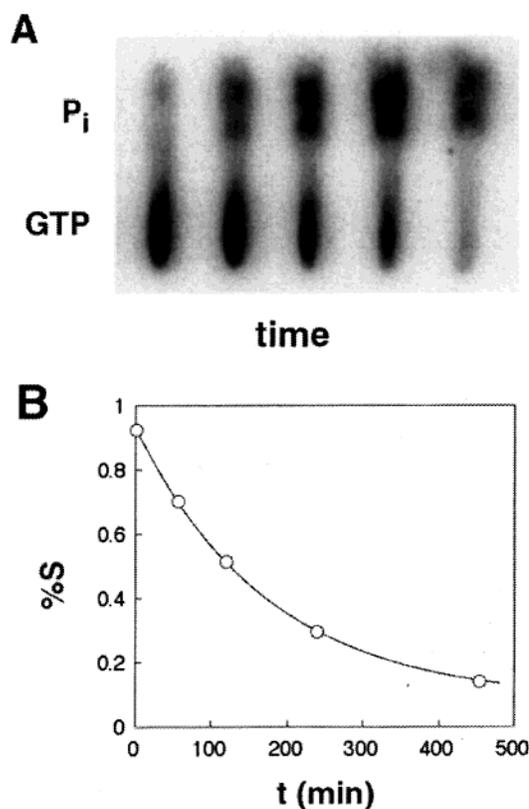
FIGURE 2: Single turnover assays for accurate determination of the low basal GTPase rates of Ffh and FtsY. (A) TLC analysis to follow the extent of a GTPase reaction, as described in Materials and Methods. A single turnover reaction of γ-^{32}P-GTP in the presence of 10 μM FtsY is shown. (B) The time course of the reaction shown in part A follows a single-exponential function. The data are fit to eq 1 (see Materials and Methods) and give an observed rate constant of 5.7 × 10^{-3} min^{-1}. In the absence of protein, GTP hydrolysis is below our detection limit over the time scale of this experiment (≤10^{-5} min^{-1}).

binding to Ffh (5 × 10^3 M^{-1} s^{-1} vs 0.9 × 10^6 M^{-1} s^{-1}; *11*), and (ii) the maximal rate constant for GTP hydrolysis, k_{max}, is 5 × 10^3-fold slower than the rate of GTP dissociation from Ffh (1.5 × 10^{-3} s^{-1} vs 7.6 s^{-1}; *11*). Therefore, $K_{1/2}$ is equal to K_1, the equilibrium dissociation constant of GTP from Ffh or Ffh•R, and k_{max} is equal to k_2, the rate constant for hydrolysis of GTP from the ^{GTP}•Ffh complex (Figure 1). These rate and equilibrium constants are summarized in Table 1.

An analogous experiment was performed for the basal GTPase reactions of FtsY (Figure 3B). Analysis of the FtsY concentration dependence gave a $K_{1/2}$ value of 14 μM and a maximal rate constant of 0.012 min^{-1} with saturating FtsY. As with Ffh, the slow basal GTPase rate and the weak GTP affinity of FtsY strongly suggest that the chemical step is rate-limiting, so that $K_{1/2}$ represents the GTP dissociation constant of FtsY (K_1') and k_{max} is the rate constant for GTP hydrolysis from the FtsY$^{•GTP}$ complex (k_2').

To obtain additional evidence that 4.5S RNA does not affect the nucleotide affinity of Ffh, the affinity of GDP for Ffh (Figure 1, K_3) was determined in the presence and absence of RNA using GDP as an inhibitor of the reaction Ffh + GTP* → products (Figure 4). The inhibition constant of GDP is the same, within error, with or without 4.5S RNA bound to Ffh (Figure 4, open and closed symbols; Table 1), indicating that 4.5S RNA does not affect the GDP affinity
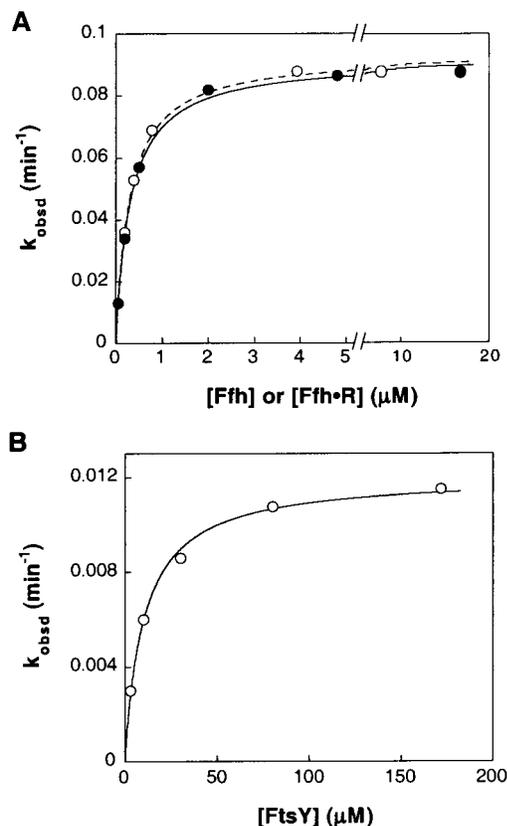
FIGURE 3: Basal GTPase reactions of Ffh and FtsY and the effect of 4.5S RNA. (A) [Ffh]-dependence of the observed rate constant of GTP hydrolysis in the presence (●) and absence (○) of 4.5S RNA, determined as in Figure 2. These concentration dependences are fit to eq 3 (see Materials and Methods) and give maximal rate constants of k_{max} = 0.92 and 0.93 min^{-1} and $K_{1/2}$ values of 0.31 and 0.30 μM in the presence and absence of 4.5S RNA, respectively. (B) [FtsY]-dependence of the observed rate constant for GTP hydrolysis. The concentration dependence is fit to eq 3 (see Materials and Methods) and gives a maximal rate constant of 0.012 min^{-1} and a $K_{1/2}$ value of 14 μM.

Table 1: Summary of Rate and Equilibrium Constants for the GTPase Cycle of Ffh and FtsY[a]

rate or equilibrium constant	−4.5S RNA	+4.5S RNA
K_1	0.30 ± 0.05 μM	0.31 ± 0.05 μM
k_2	0.093 ± 0.002 min^{-1}	0.092 ± 0.002 min^{-1}
K_3	0.20 ± 0.10 μM	0.32 ± 0.08 μM
K_1'	14 ± 2 μM	n.a.[c]
k_2'	0.012 ± 0.002 min^{-1}	n.a.[c]
K_3'	26 ± 2 μM	n.a.[c]
k_4	5.6($\pm$0.3) × 10^3 M^{-1} s^{-1}	1.8($\pm$0.1) × 10^6 M^{-1} s^{-1}
k_{-4}	1.2($\pm$0.1) × 10^{-5} s^{-1b}	3.3($\pm$0.6) × 10^{-3} s^{-1b}
k_5	0.12 ± 0.01 s^{-1}	0.71 ± 0.03 s^{-1}
k_6	≥0.12 s^{-1d}	≥0.71 s^{-1d}

[a] The rate and equilibrium constants are defined in Figure 1. [b] Values of k_{-4} were determined with GppNHp (35). It is possible that the values with GTP are different, as there is a 10-fold faster association rate constant between Ffh and FtsY (k_4) with GTP than with GppNHp as the bound nucleotide. [c] n.a., not applicable as FtsY does not measurably interact with 4.5S RNA. [d] Only lower limits can be estimated for the values of k_6, because product dissociation has not been directly measured and because these steps are most likely faster than k_5 (see text).

of Ffh either. The results in this section provide strong evidence that 4.5S RNA does not affect the basal GTPase reaction of Ffh.
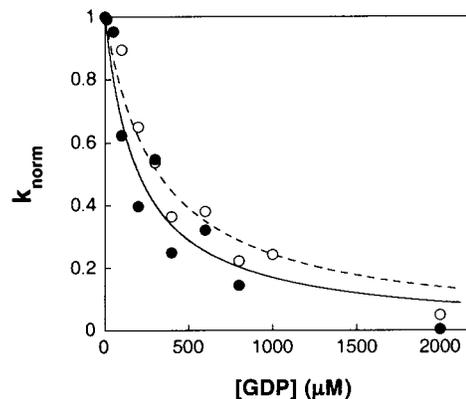
FIGURE 4: 4.5S RNA has no effect on the affinity of GDP for Ffh. The observed rate constant for the reaction GTP* + Ffh → products ([Ffh] = 0.05 μM) was determined at varying GDP concentrations in the presence (●) and absence (○) of 4.5S RNA. The observed rate constants are normalized such that k_{norm} = 1 in the absence of added GDP. The [GDP]-dependences are fit to eq 4, as described in Materials and Methods, and give inhibition constants of K_i = 0.32 and 0.20 μM in the presence and absence of 4.5S RNA, respectively.

4.5S RNA Accelerates the Association between Ffh and FtsY in Their GTP-Bound Forms. In previous work, we demonstrated that 4.5S RNA accelerates the association between Ffh and FtsY (35). In this earlier work, the Ffh•FtsY complex was trapped using the nonhydrolyzable GTP analogue GppNHp, and complex formation was monitored using a fluorescence assay that follows the increase in the intrinsic tryptophan fluorescence of FtsY upon association with Ffh (12, 35). To know whether the stimulatory effect of 4.5S RNA occurred with the GTP-bound form of the proteins, we used this fluorescence assay to determine the rate constant for association of ^{GTP}•Ffh with FtsY•^{GTP} in the presence and absence of 4.5S RNA.[4]

4.5S RNA increases the rate constant for association of Ffh with FtsY in their GTP-bound forms by 400-fold, from 5.6 × 10^3 M^{-1} s^{-1} to 1.8 × 10^6 M^{-1} s^{-1} (Figure 5; Figure 1, k_4). This effect is similar to the 200-fold acceleration of Ffh−FtsY association by 4.5S RNA with GppNHp bound to the proteins (35). Interestingly, these association rate constants are ∼10-fold faster with GTP than with GppNHp both in the presence and absence of RNA, indicating that formation of the Ffh•FtsY complex is sensitive to the chemical nature of the bridging atom between the β- and γ-phosphate.

GTP Hydrolysis from ^{GTP}•Ffh•FtsY•^{GTP} Is Faster than Dissociation of the Complex. Previously, we have found that 4.5S RNA also accelerates dissociation of the Ffh•FtsY complex in the GppNHp-bound form (35). To ask whether

[4] There is substantial evidence that the fluorescence change of FtsY in the presence of Ffh and GTP (or GppNHp) arises from Ffh−FtsY association, not from GTP binding to FtsY in the presence of Ffh. First, in the absence of Ffh, GTP does not produce the large fluorescence change in FtsY as observed in the presence of Ffh (12) and results not shown). Second, the high concentration of GTP used in the experiment of Figure 5 (1 mM) ensures that GTP binds to FtsY much faster than the observed rate of Ffh-FtsY association ($k_{on,app}^{GTP}$ = 800 s^{-1} vs $k_{on,app}^{Ffh}$ ≤ 14 s^{-1}; $k_{on,app}^{GTP}$ = k_{on}^{GTP} × [GTP]; $k_{on,app}^{Ffh}$ = k_{on}^{Ffh} × [Ffh]). Finally, experiments in which GTP is prebound to FtsY and complex formation is initiated by addition of Mg^{2+} yielded the same fluorescence change. We therefore attribute the FtsY fluorescence change to GTP-dependent complex formation between Ffh and FtsY.

A

B

C
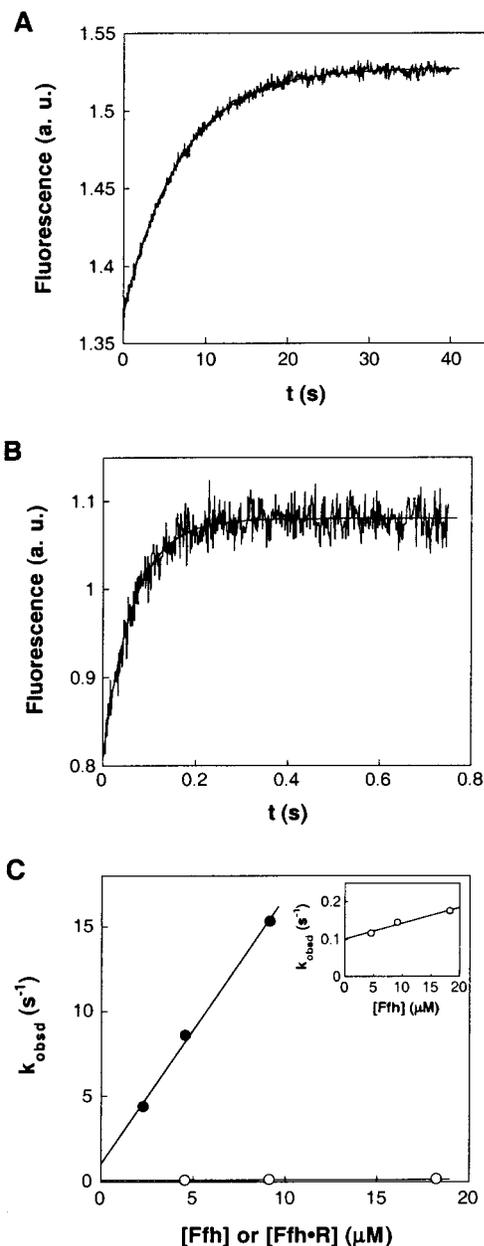
FIGURE 5: 4.5S RNA accelerates formation of the complex between ^{GTP}•Ffh and FtsY•^{GTP}. The time course for formation of the ^{GTP}•Ffh•FtsY•^{GTP} complex was monitored by the increase in FtsY tryptophan fluorescence in the absence (A) and presence (B) of 4.5S RNA, shown for the reactions in the presence of 0.5 μM FtsY and 9.1 μM Ffh. These time courses are fit to single-exponential functions analogous to eq 1 in Materials and Methods and give observed rate constants of 0.15 and 15 s^{-1} in the absence and presence of 4.5S RNA, respectively. Note the difference in time scales for the reactions in parts A and B. (C) [Ffh]-dependence of the observed association rate constants in the presence of 0.5 μM FtsY with ($\bullet$) and without ($\circ$) 4.5S RNA present. The inset shows the data in the absence of 4.5S RNA on an expanded scale. The lines are fits of the data to eq 5 in Materials and Methods, which give association rate constants of $k_4 = 5.6 \times 10^3$ and 1.8×10^6 M^{-1} s^{-1} in the absence and presence of 4.5S RNA, respectively, and intercepts of $(k_{-4} + k_5) = 1.0$ and 0.10 s^{-1} in the presence and absence of 4.5S RNA, respectively.

the same effect also holds with GTP bound to the proteins, a pulse-chase experiment was carried out to determine the rate of disassembly of the ^{GTP}•Ffh•FtsY•^{GTP} complex, which can be monitored by decay of the fluorescence signal from this complex (see Materials and Methods). Unlike the
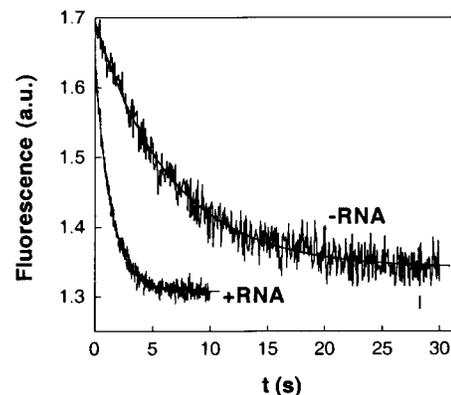
FIGURE 6: The effect of 4.5S RNA on the rate of apparent disassembly of the ^{GTP}•Ffh•FtsY•^{GTP} complex, measured by pulse-chase experiments as described in Materials and Methods. The data are fit to eq 6b (see Materials and Methods), which give apparent rate constants of 0.15 and 0.72 s^{-1} in the absence and presence of 4.5S RNA, respectively.

previous observations, however, disassembly of the complex occurs with apparent rate constants of 0.15 and 0.72 s^{-1} in the absence and presence of 4.5S RNA, respectively[5] (Figure 6). These rate constants are more than 200-fold faster than the dissociation rates of the ^{GppNHp}•Ffh•FtsY•^{GppNHp} complex previously observed (35). In addition, the effect of 4.5S RNA is much smaller, only 5-fold, in contrast to the 300-fold acceleration of complex dissociation by 4.5S RNA in the presence of GppNHp (35).

One explanation for these discrepancies is that decay of the fluorescence signal occurs not because of dissociation of the ^{GTP}•Ffh•FtsY•^{GTP} complex (k_{-4}), but rather because GTP is hydrolyzed to yield the ^{GDP}•Ffh•FtsY•^{GDP} complex (k_5), which rapidly dissociates and does not give a fluorescence signal (35). This model can be tested by directly measuring the rate of GTP hydrolysis by the Ffh•FtsY complex and determining the effect of 4.5S RNA on this reaction. According to this model, the rate of GTP hydrolysis from the ^{GTP}•Ffh•FtsY•^{GTP} complex would be the same as the apparent rate of complex disassembly (Figure 6). Further, the 4.5S RNA would be predicted to have the same effect on this rate as that observed in Figure 6.

The rate constant for GTP hydrolysis was determined in the presence of a fixed small amount of Ffh and varying concentrations of FtsY (Figure 7). The concentration of FtsY was varied because its lower basal GTPase activity allows us to observe the reaction from the complex over a wider FtsY concentration range without interference from its basal GTPase reaction. Multiple turnover, instead of single turnover, experiments needed to be used to measure the stimulated GTPase reaction in the presence of both Ffh and FtsY, because interaction of Ffh with FtsY requires GTP bound to both proteins and because Ffh and FtsY have weak GTP affinities (Table 1, K_1 and K_1', respectively). Therefore, a high concentration of GTP in excess of the proteins was

---

[5] Alternatively, the rate constant for decay of the ^{GTP}•Ffh•FtsY•^{GTP} complex, which is equal to $k_{-4} + k_5$ (eq 4 in the Materials and Methods), can also be obtained from extrapolation of the Ffh concentration dependence of the observed association rate constants to zero (Figure 5). The y-intercept thus obtained is 1.0 and 0.10 s^{-1} in the presence and absence of 4.5S RNA, respectively, in close agreement with the values obtained from the pulse-chase experiment.
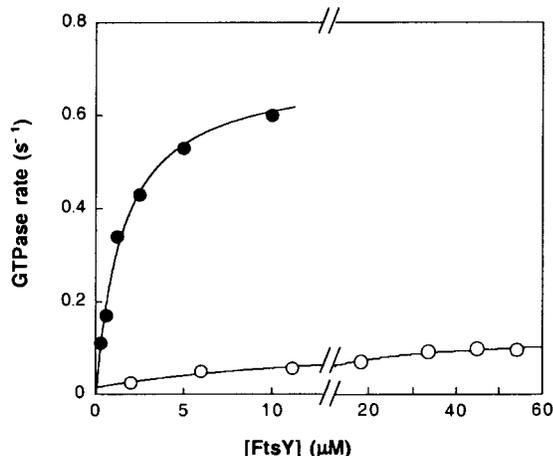
FIGURE 7: 4.5S RNA increases the rate of GTP hydrolysis from the ^{GTP}·Ffh·FtsY·^{GTP} complex. The observed rate constant for the stimulated GTPase reactions is determined with a small fixed amount of Ffh and varying concentrations of FtsY in the presence (●) and absence (○) of 4.5S RNA (0.1 and 0.5 μM Ffh with and without RNA present, respectively), as described in Materials and Methods. The data are fit to eq 3 (see Materials and Methods), which give maximal rate constants of 0.71 and 0.12 s^{-1} and $K_{1/2}$ values of 1.6 and 11 μM in the presence and absence of 4.5S RNA, respectively.

FIGURE 8: The time course of GTP hydrolysis from the Ffh·FtsY complex shows no obvious burst phase. The reaction was carried out in the presence of 20 μM Ffh, 79 μM FtsY, and 250 μM GTP; the high concentration of Ffh/FtsY relative to GTP is used to maximize the chance of observing the presence of a burst phase, as described in the text. The different symbols represent data from two independent experiments. The solid line is a fit of the initial part of the time course to a single-exponential function (eq 1 in Materials and Methods). The dashed lines are fits of the data to models in which a faster burst phase during the first turnover is followed by a slower steady-state rate (eq 2 in Materials and Methods), with the reaction rate during the burst phase (k_1) fixed at different values relative to the steady-state rate (k_2): $k_1 = 5k_2$ (− − −); $k_1 = 10k_2$ (···); $k_1 = 20k_2$ (− · − · −).

present to ensure that both proteins are in their GTP-bound forms.

The rate constant for the stimulated GTPase reaction increases with increasing FtsY below 1 μM FtsY and saturates at higher concentrations (Figure 7). The maximal rate constants with saturating FtsY (k_{max}), which represent the rate constants for hydrolysis of GTP from the ^{GTP}·Ffh·FtsY·^{GTP} complex (k_5; see below for justification that $k_{max} = k_5$), are 0.71 and 0.12 s^{-1} in the presence and absence of 4.5S RNA, respectively. These rate constants are the same, within error, as the apparent rate constants for disassembly of the ^{GTP}·Ffh·FtsY·^{GTP} complex of 0.72 and 0.15 s^{-1} observed in Figure 6. These results provide strong evidence that disappearance of the fluorescence signal from the ^{GTP}·Ffh·FtsY·^{GTP} complex in Figure 6 proceeds through hydrolysis of GTP from the complex (k_5), which is faster than dissociation of the ^{GTP}·Ffh·FtsY·^{GTP} complex (k_{-4}). Further, these results suggest that 4.5S RNA has an additional effect on the rate constant for hydrolysis of GTP once the ^{GTP}·Ffh·FtsY·^{GTP} complex is formed.

Because multiple turnover reactions were monitored in this experiment, it is possible that steps after GTP hydrolysis, such as dissociation of the ^{GDP}·Ffh·FtsY·^{GDP} complex (k_6), are rate-limiting for the reaction ^{GTP}·Ffh·FtsY·^{GTP} → products and that 4.5S RNA affects the product release steps instead of the GTP hydrolysis rate. This possibility is tested in the experiments described below.

Product Dissociation Is Not Rate-Limiting for the GTPase Reaction of the Ffh·FtsY Complex. To test whether steps before or after GTP hydrolysis are rate-limiting, the time course for the reaction ^{GTP}·Ffh·FtsY·^{GTP} → products was monitored at sufficiently high Ffh and FtsY concentrations relative to GTP, so that the presence of a burst phase could be readily detected. If steps after GTP hydrolysis were rate-limiting, then a burst of product formation followed by a slower reaction would be predicted. In contrast, a burst phase

would not be observed if steps prior to GTP hydrolysis were rate-limiting.

Under these conditions, the initial time course for the GTPase reaction of the Ffh·FtsY complex is consistent with a single-exponential rate without exhibiting a burst phase (Figure 8, solid line). To explore under what situations a burst phase would be observed, the time course was fit to models in which there is a burst phase during the first turnover followed by a slower steady-state rate (Figure 8, dashed lines). The analysis indicates that significant deviations from the data would be observed if the rate constant during the burst phase (k_6) is ≥5-fold faster than the steady-state rate constant. Thus, the rate constant for product release is at least within 5-fold of that for the steps prior to GTP hydrolysis.

The following observations provide additional evidence that product dissociation is not likely to be rate-limiting. In single turnover experiments with a xanthosine triphosphate (XTP)-specific mutant of FtsY, FtsYD449N (*10*), the rate constant for XTP hydrolysis in the reaction ^{GppNHp}·Ffh·FtsYD449N·^{XTP} → products is similar to the maximal rate of GTP hydrolysis observed in the multiple turnover reactions above (Shan, S., unpublished results). In contrast, a much faster single turnover rate would be observed if product release were rate-limiting. In addition, previous work has shown that GDP dissociation from Ffh and FtsY is fast, with rate constants of 14 and 5 s^{-1}, respectively (*11−13*), so that GDP release is not likely to be rate-limiting. Further, the affinities of Ffh and FtsY for inorganic phosphate (P$_i$) are weak, with dissociation constants in the millimolar range even in the presence of GDP (data not shown), suggesting that P$_i$ dissociation is also unlikely to be rate-limiting. Finally, there is strong evidence that a stable Ffh·FtsY complex does not appear to form with GDP as the bound nucleotide, even
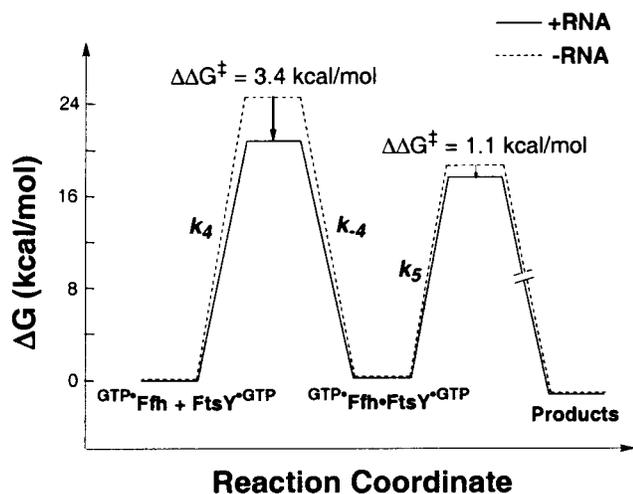
FIGURE 9: Free-energy profile for the GTPase cycle upon interaction of Ffh with FtsY in the presence (solid line) and absence (dashed line) of 4.5S RNA. The individual rate constants are defined in Figure 1. The relative energy levels are shown for a standard state of 1 nM and were calculated from the rate constants in Table 1 using the equation $\Delta G = -RT \ln(kh/k_B T)$, in which $R = 1.987$ cal mol^{-1} K^{-1}, $k_B = 3.3 \times 10^{-24}$ cal K^{-1}, $h = 1.58 \times 10^{-34}$ s, and $T = 298$ K. Note that the free energy levels for the ^{GTP}Ffh·FtsY^{GTP} complex are estimated from dissociation rate constants of the Ffh·FtsY complex previously determined with GppNHp; the values for GTP are likely to be different, as described in the legend to Table 1.

in the presence of millimolar concentrations of P_i, suggesting that dissociation of $^{GDP \cdot P_i}$Ffh from FtsY$^{GDP \cdot P_i}$ is also fast and unlikely to be rate-limiting. Although a rate-limiting product release cannot be ruled out, all of the results obtained here and previously are consistent with the model that steps prior to GTP hydrolysis (k_5) are rate-limiting for the reaction ^{GTP}Ffh·FtsY$^{GTP} \rightarrow$ products. It is therefore unlikely that the observed effect of 4.5S RNA arises from an effect on the product release steps.

DISCUSSION

In this work, mechanistic analyses of the effects of 4.5S RNA on the GTPase cycles of Ffh and FtsY have provided insights into the role of 4.5S RNA in SRP-mediated targeting. The results also establish a framework that allows us to understand previous observations and to design and interpret future experiments.

To understand the role of a molecule in a biological process, it is crucial to know the thermodynamic and kinetic features of the process. The rate and equilibrium constants for the individual reaction steps described herein have allowed us to interpret the effects of 4.5S RNA in a unifying model that reconciles all of the previous observations (e.g., 20, 34, 35). Figure 9 shows a free-energy profile for the GTPase reaction upon interaction of Ffh with FtsY and summarizes the roles of 4.5S RNA in this reaction. The major effect of 4.5S RNA is to accelerate the formation of the ^{GTP}Ffh·FtsY^{GTP} complex 400-fold, as described herein and in previous work (35; Figure 9, thick arrow). Importantly, dissociation of the ^{GTP}Ffh·FtsY^{GTP} complex is slower than hydrolysis of GTP from this complex (Figure 9, $k_5 > k_{-4}$). Thus, with subsaturating proteins the association of Ffh with FtsY, rather than the chemical step of GTP hydrolysis, is the rate-limiting step for the observed GTPase reaction

(Figure 9, k_4). This can account for the previously observed requirement of 4.5S RNA in the targeting reaction in vivo and the apparent stimulatory effect of this RNA on the GTPase reactions in the presence of both proteins in vitro (e.g. 20, 34).

Interestingly, the rate of complex formation with GTP bound to the proteins is 10-fold faster than previously observed with GppNHp bound, both in the presence and absence of 4.5S RNA, suggesting that complex formation is sensitive to the chemical nature of the atom bridging the β- and γ-phosphate of GTP. Consistent with this, GTPγS, in which one of the nonbridging phosphate oxygens of the γ-phosphate group is replaced by sulfur, does not support formation of a stable Ffh·FtsY complex as does GTP or GppNHp (unpublished results), suggesting that interactions with the nonbridging γ-phosphate oxygens are also crucial for formation of the complex. These observations strongly suggest that multiple interactions are made with the γ-phosphate group to provide the energetic driving force for complex formation. In contrast, the GTP and GDP affinities are indistinguishable for both Ffh and FtsY in their uncomplexed form, suggesting that no substantial interactions are made with the γ-phosphate group prior to complex formation. Together, these results strongly suggest that conformational changes involving residues surrounding the γ-phosphate occur within the GTPase active site of Ffh and/or FtsY upon interaction with one another. This is analogous to the regulatory mechanism of many other ATPase and GTPase proteins, in which the presence of the γ-phosphate group acts as a switch to induce conformational changes of the protein that turns the protein into its active form (e.g., 15, 39 and references therein).

An additional step, GTP hydrolysis from the ^{GTP}Ffh·FtsY^{GTP} complex, is also moderately accelerated by 4.5S RNA (Figure 9, arrow in the peak on the right side). This effect suggests that 4.5S RNA also helps to form a more reactive conformation within the Ffh·FtsY complex that is conducive to GTP hydrolysis. It should be noted, however, that the reaction ^{GTP}Ffh·FtsY$^{GTP} \rightarrow$ products could still be limited by a conformational rearrangement within the complex or by the chemical step of GTP hydrolysis. It remains to be determined whether the observed effect of 4.5S RNA on this reaction arises from its stimulatory effect on the chemical reaction or from a catalytic effect on a conformational change within the complex analogous to its role in complex formation described here and previously (35).

The catalytic role of 4.5S RNA in mediating the interaction between Ffh and FtsY suggests that this molecule could serve as a regulatory factor for the SRP targeting cycle. The results herein describe differences in the presence and absence of 4.5S RNA. In vivo, however, 4.5S RNA would be bound to Ffh throughout the targeting cycle because of the tight Ffh—RNA association and because the affinity of Ffh for 4.5S RNA does not appear to be altered by additional components in the targeting pathway such as nucleotides, the SRP receptor, or the ribosome·nascent chain complex (12, 35; results herein and Johnson, A. E., personal communication). Nevertheless, the function of this RNA could be regulated by additional components in the targeting pathway. Recent work showed that mutations in a conserved tetraloop region of 4.5S RNA disrupt the interaction of Ffh with FtsY (33), supporting the possibility that the function of this RNA can

be subject to modulation. 4.5S RNA binds to the M-domain of Ffh, which also contains the binding site for signal sequences. Crystallographic analyses of the M-domain structure showed that the SRP RNA is positioned close to the signal sequence binding pocket, suggesting communication between the RNA and signal sequences (*28*). Thus, it could be envisioned that the presence of a signal sequence or the ribosome could modulate the activity of 4.5S RNA, thereby turning this molecule into an active regulator of the SRP targeting process. The kinetic and thermodynamic framework established in this work will facilitate the characterization of potential effectors, such as signal sequences, ribosome, and the translocation machinery, on the GTPase cycles of Ffh and FtsY and aid in determining whether and how the function of 4.5S RNA is modulated by these components during the targeting cycle.

REFERENCES

1. Walter, P. and Johnson, A. E. (1994) *Annu. Rev. Cell Biol. 10*, 87−119.
2. Walter, P., Ibrahimi, I., and Blobel, G. (1981) *J. Cell. Biol. 91*, 545−550.
3. Gilmore, R., Blobel, G., and Walter, P. (1982a) *J. Cell Biol. 95*, 463−469.
4. Gilmore, R., Walter, P., and Blobel, G. (1982b) *J. Cell Biol. 95*, 470−477.
5. Walter, P. and Blobel, G. (1981) *J. Cell Biol. 91*, 557−561.
6. Bernstein, H. D., Poritz, M. A., Strub, K., Hoben, P. J., Brenner, S., and Walter, P. (1989) *Nature 340*, 482−486.
7. Bernstein, H. D., Zopf, D., Freymann, D. M., and Walter, P. (1993) *Proc. Natl. Acad. Sci. U.S.A. 90*, 5229−5234.
8. Römisch, K., Webb, J., Lingelback, K., Gausepohl, H., and Dobberstein, B. (1990) *J. Cell Biol. 111*, 1793−1807.
9. Zopf, D., Bernstein, H. D., Johnson, A. E., and Walter, P. (1990) *EMBO J. 9*, 4511−4517.
10. Powers, T. and Walter, P. (1995) *Science 269*, 1422−1424.
11. Jagath, J. R., Rodnina, M. V., Lentzen, G., and Wintermeyer, W. (1998) *Biochemistry 37*, 15408−15413.
12. Jagath, J. R., Rodnina, M. V., and Wintermeyer, W. (2000) *J. Mol. Biol. 295*, 745−753.
13. Moser, C., Mol, O., Goody, R. S., and Sinning, I. (1997) *Proc. Natl. Acad. Sci. U.S.A. 94*, 11339−11344.
14. Gilmore, R., and Hoffman, K. E. (1988) *J. Biol. Chem. 263*, 4381−4385.
15. Bourne, H. R., Sanders, D. A., and McCormick, F. (1991) *Nature 349*, 117−127.
16. Freymann, D. M., Keenan, R. J., Stroud, R. M., and Walter, P. (1997) *Nature 385*, 361−364.
17. Montoya, G., Svensson, C., Luirink, J., and Sinning, I. (1997) *Nature 385*, 365−368.
18. Zopf, D., Bernstein, H. D., and Walter, P. (1993) *J. Cell Biol. 120*, 1113−1121.
19. Miller, J. D., Wilhelm, H., Gierasch, L., Gilmore, R., and Walter, P. (1993) *Nature 366*, 351−354.
20. Miller, J. D., Bernstein, H. D., and Walter, P. (1994) *Nature 367*, 657−659.
21. Connolly, T., and Gilmore, R. (1989) *Cell 57*, 599−610.
22. Connolly, T., Rapiejko, P. J., and Gilmore, R. (1991) *Science 252*, 1171−1173.
23. Zelazny, A., Seluanov, A., Cooper, A., and Bibi, E. (1997) *Proc. Natl. Acad. Sci. U.S.A. 94*, 6025−6029.
24. Powers, T., and Walter, P. (1997) *EMBO J. 16*, 4880−4886.
25. de Leeuw, E., te Kaat, K., Moser, C., Memestrina, G., Demel, R., de Kruijff, B., Oudegam, B., Luirink, J., and Sinning, I. (2000) *EMBO J. 19*, 531−541.
26. Lütcke, H., High, S., Römisch, K., Ashford, A. J., and Dobberstein, B. (1992) *EMBO J. 11*, 1543−1551.
27. Keenan, R. J., Freymann, D. M., Walter, P., and Stroud, R. M. (1998) *Cell 94*, 181−191.
28. Batey, R. T., Rambo, R. P., Lucast, L., Rha, B., and Doudna, J. A. (2000) *Science 287*, 1232−1239.
29. Walter, P., and Blobel, G. (1982) *Nature 299*, 691−698.
30. Poritz, M. A., Strub, K., and Walter, P. (1988) *Cell 55*, 4−6.
31. Struck, C. R. J., Toschka, H. Y., Specht, T., Erdmann, V. A. (1988) *Nucleic Acids Res. 16*, 7740−7746.
32. Lentzen, G., Moine, H., Ehresmann, C., Ehresmann, B., and Wintermeyer, W. (1996) *RNA 2*, 244−253.
33. Jagath, J. R., Matassova, N. B., de Leeuw, E., Warnecke, J. M., Lentzen, G., Rodnina, M. V., Luirink, J., and Wintermeyer, W. (2001) *RNA 7*, 293−301.
34. Macao, B., Luirink, J., and Samuelsson, T. (1997) *Mol. Microbiol. 24*, 523−534.
35. Peluso, P., Herschlag, D., Nock, S., Freymann, D. M., Johnson, A. E., and Walter, P. (2000) *Science 288*, 1640−1643.
36. Brown, S., and Fournier, M. J. (1984) *J. Mol. Biol. 178*, 533−550.
37. Sambrook, J., Fritsch, E. F., Maniatis, T. (1989) in *Molecular Cloning: A Laboratory Manual*, Cold Spring Harbor Laboratory Press, Plainview, NY.
38. Rose, I. A., O'Connell, E. L., Litwin, S., and Bar Tana, J. (1974) *J. Biol. Chem. 249*, 5163−5168.
39. Lorsch, J. R., and Herschlag, D. (1998) *Biochemistry 37*, 2194−2206.

BI011639Y